

# COMPUTATIONAL MODELING OF PROTOCELL DIVISION: A SPATIALLY EXTENDED METABOLISM-MEMBRANE SYSTEM

Javier Macia<sup>[1]</sup> and Ricard V. Solé<sup>[1,2]</sup>

[1] ICREA-Complex Systems Lab, Universitat Pompeu Fabra,  
Dr Aiguader 80, 08003 Barcelona (Spain)

[2]Santa Fe Institute, 1399 Hyde Park Road, Santa Fe NM87501, USA

## Abstract

**Cellular life requires the presence of a set of biochemical mechanisms in order to maintain a predictable process of growth and division. Cell division modeling is known to be a hard computational problem. Even when using a small number of assumptions, realistic simulations are often computationally costly and simplified ones far from realistic. In this paper we present a simple lattice-based model of cell replication involving a discrete semi-permeable membrane with an internal minimal metabolism involving two reactive centers. It is shown that such a system can effectively lead to a whole cell replication cycle. The model can be used as a basic framework to model whole protocell dynamics including more complex sets of reactions.**

## INTRODUCTION

Membranes take part in many of the essential processes involved in the maintenance of cellular life (Albert et al., 2005; Lodish et al, 2005). They define the boundaries separating the inside world of chemical reactions and information from the outside environment. They play a very important role in exchanging substances with the external medium and in the growth and later cellular division. Current cells are very complex, as a result of a long evolutionary process, and have sophisticated mechanisms for cellular division regulation. However, the analysis of minimal cellular structures can contribute to a better understanding of possible prebiotic scenarios in which cellular life could have originated (Maynard Smith and Szathmáry, 2001) as well as in the design and synthesis of new artificial protocells (Rasmussen et al., 2004) .

A first approximation to a minimal cell structure is to consider a simplified model including the essential membrane physics defined in terms of the average behavior of a continuous, closed system involving some sort of simple, internal metabolism. Membrane division can take place spontaneously when membrane size goes beyond a critical value. In this case, the division process becomes energetically favored (Noguchi and Takasu, 2002; Schaff et al., 2001). However, cell division can be also actively induced through different mechanisms (Schaff et al., 2001, White 1980). Understanding how these mechanisms trigger cell division can be very useful in designing of artificial protocells. Early work in this area was done by Rashevsky, who mathematically explored the conditions under which a single cell could experience a

process of membrane expansion, deformation and splitting (Rashevsky, 1960). Given the lack of available computational resources at the time, the analysis was largely based on mathematical approximations.

An important component of a spatially-extended physically and chemically consistent model of protocell replication requires a minimal set of rules preserving the underlying chemistry and physics. In this context, Morgan et al. have developed well-defined framework to the growth and division process as a non-stationary phenomenon (Morgan et al., 2004). In such approximation, the biochemistry is coupled to a spatially-implicit container, where the effects of cell geometry are introduced by means of scaling considerations. Some related approximations have been recently used in relation with the chemoton model (Munteanu and Solé, 2005). However, it would be also desirable to model cell replication under spatially-explicit conditions. This is particularly important in order to understand possible internal mechanisms triggering destabilization of closed membranes. Realistic models involving stochastic particle models (Ono and Ikegami, 1999) molecular dynamics (or dissipative particle dynamics) methods are not yet fully developed, and they are rather computationally expensive (see Solé et al, 2006 and references therein). In these frameworks, each molecule (or some simplified representation of it as a particle) is explicitly modeled, with physical interactions taking place at the microscopic scale. This is especially relevant when dealing with nano-scale systems, but becomes less needed when dealing with lipid vesicles. Some current approaches to the synthesis of artificial cells are actually based on the use of a large vesicle as a container (Hanczyc et al., 2003; Hanczyc and Szostak, 2004; see also Szostak et al., 2001 for a review and references therein).

Among different possibilities of modeling spatial vesicles, the effects of time- and space-variable osmotic pressures seems one of the most suitable mechanisms inducing membrane division, since this variable pressures can be generated by the internal metabolism, without external elements. What is required here is an active, non-equilibrium process able to trigger the growth the protocell. Provided that the interplay between metabolism and membrane geometric changes are able to trigger a symmetric deformation, cell division might be spontaneously achieved. In this paper we analyze how a simple metabolism can create such variable osmotic pressures and how the membrane becomes deformed under such differential pressures until completing division. For simplicity we restrict ourselves to a two-dimensional scenario.

## METABOLISM AND OSMOTIC PRESSURES

### Metabolic reactions:

Several possible implementations of a self-replicating cell can be constructed. Here we present one of them, leaving a general clarification to a future work. The object of study is a minimal cellular structure, formed by a closed continuous membrane enclosing a set of metabolic reactions. Some of these reactions need the presence of two *metabolic centers* (enzymes)  $E_1$  and  $E_2$  adhered to the internal face of the membrane (see figure 1). This assumption is actually close to those performed by Rashevsky, although they can be relaxed under some conditions (Macia and Solé, in preparation). These elements act as catalysts of these metabolic reactions:



These enzymes might be specifically designed molecules including several catalytic centers (two in this case). Additional metabolic reactions are included, namely:



where  $S_1$ ,  $S_2$  y  $G'_0$  are non-reactive, waste substances.

Furthermore, other metabolic reactions synthesize basic membrane elements  $M$  from a reactive precursor  $L$ . These  $M$  molecules are the building blocks for membrane growth and are directly incorporated into the membrane as fast as produced in the metabolic centers  $E_1$  and  $E_2$ .



The substances  $R$  and  $L$  are externally provided and available in the external medium. They are continuously pumped from a source located at the limits of the system, and cross de membrane by diffusion, with permeabilities  $h_R$  and  $h_L$ , respectively. Similarly, all the substances produced in the metabolic reactions diffuse outwards crossing the membrane with perm abilities  $h_{G_1}$ ,  $h_{G_2}$ ,  $h_{S_1}$ ,  $h_{S_2}$ ,  $h_{G_0}$  and  $h_{G'_0}$ , respectively.

Since some of these reactions take place within a finite space domain (where the metabolic centers  $E_1$  and  $E_2$  are located) the distribution of the different substances is not uniform in the space. These spatially-localized reactions are the origin of non-uniform osmotic pressures along the membrane. On the other hand, due to these non-uniform osmotic pressures the membrane can become deformed and the location of the metabolic centers adhered to the internal side of the membrane can change along time. The combination of these two effects is the origin of time and space variable pressures.

Finally, the model assumes that in the external zone there is a substance that inhibits the reaction (1.3). This substance cannot cross the membrane and has a constant concentration, enough to guarantee that basically the production of  $G_0$  takes place inside the membrane. Reaction (1.4) is not essential to obtain cell division. However, this reaction acts as a mechanism to remove  $G_0$  and to increase the osmotic pressure associated to  $R$  in the narrowed zone. In this sense, it allows to accelerate the fission process in a rather efficient way.

All the concentrations are time and space dependent. For a given molecule  $x$ , its concentration will be  $c_x \equiv c_x(\mathbf{r}, t)$ , with  $\mathbf{r} = (r_1, r_2)$  indicating the spatial coordinates. For notational simplicity, this dependence is not explicitly written. The reaction-diffusion equations are given by:

$$\frac{\partial c_{G_1}}{\partial t} = 2 \cdot k_1 \cdot c_R \cdot c_{E_1} + k_{-3} \cdot c_{G_0} - k_3 \cdot c_{G_1} \cdot c_{G_2} D_{G_1} \nabla^2 c_{G_1} \quad (2.1)$$

$$\frac{\partial c_{G_2}}{\partial t} = 2 \cdot k_2 \cdot c_R \cdot c_{E_2} + k_{-3} \cdot c_{G_0} - k_3 \cdot c_{G_1} \cdot c_{G_2} + D_{G_2} \nabla^2 c_{G_2} \quad (2.2)$$

$$\frac{\partial c_{S_1}}{\partial t} = k_1 \cdot c_R \cdot c_{E_1} + D_{S_1} \nabla^2 c_{S_1} \quad (2.3)$$

$$\frac{\partial c_{S_2}}{\partial t} = k_2 \cdot c_R \cdot c_{E_2} + D_{S_2} \nabla^2 c_{S_2} \quad (2.4)$$

$$\frac{\partial c_{G_0}}{\partial t} = k_3 \cdot c_{G_1} \cdot c_{G_2} - k_{-3} \cdot c_{G_0} - k_4 \cdot c_{G_0} \cdot c_R^2 + k_{-4} \cdot c_{G'_0} + D_{G_0} \nabla^2 c_{G_0} \quad (2.5)$$

$$\frac{\partial c_{G'_0}}{\partial t} = k_4 \cdot c_{G_0} \cdot c_R^2 - k_{-4} \cdot c_{G'_0} + D_{G'_0} \nabla^2 c_{G'_0} \quad (2.6)$$

$$\frac{\partial c_R}{\partial t} = R_0 - k_1 \cdot c_R \cdot c_{E_1} - k_2 \cdot c_R \cdot c_{E_2} - 2 \cdot c_{G_0} \cdot c_R^2 + 2 \cdot c_{G'_0} + D_R \nabla^2 c_R \quad (2.7)$$

$$\frac{\partial c_L}{\partial t} = L_0 - k_5 \cdot c_L \cdot c_{E_1} - k_6 \cdot c_L \cdot c_{E_2} + D_L \nabla^2 c_L \quad (2.8)$$

Here  $D_{G1}$ ,  $D_{G2}$ ,  $D_{S1}$ ,  $D_{S2}$ ,  $D_{G0}$ ,  $D_R$  and  $D_L$  are the diffusion coefficients. In a first approximation, the model assumes that the values of these coefficients are the same inside and outside the membrane.  $R_0$  and  $L_0$  are the constant supply of  $R$  and  $L$  in the external medium. The different flows through the membrane must satisfy the boundary condition:

$$D_x \cdot \frac{\partial c_x^e(r, t)}{\partial \nu} = D_x \cdot \frac{\partial c_x^i(r, t)}{\partial \nu} = h_x \cdot (c_x^i(r, t) - c_x^e(r, t)) \quad (3)$$

where the index  $x$  corresponds to the different substances:  $x = \{G_1, G_2, S_1, S_2, G_0, G'_0, R, L\}$ ,  $c_x^e$  is the concentration of the substance  $x$  outside and  $c_x^i$  is the concentration inside the membrane.  $h_x$  is the permeability of the substance  $x$  (defined as the rate at which

molecules cross the membrane) and  $\nu$  is the normal direction to the membrane at the point  $r$ , at time  $t$ .

### Osmotic pressures and surface tension:

The flows of the different substances generate different osmotic pressures on the membrane. At each point the osmotic pressure value  $P_x^o$  generated by the substance  $x$  depends on the different concentrations of this substance at each side of the membrane:

$$P_x^o(r, t) = k_x \cdot (c_x^i(r, t) - c_x^e(r, t)) \quad (4)$$

Here  $k_x$  is constant. For the particular case of very low concentrations, we have  $k_x \approx R \cdot T$ , where  $R$  is the ideal gas constant and  $T$  is the temperature (if the concentrations are expressed in mols/liter). The osmotic pressure at one point  $r$  of the membrane at time  $t$  can be calculated by adding the pressure generated by each substance, as follows:

$$P_t^o(r, t) = \sum_x k_x \cdot (c_x^i(r, t) - c_x^e(r, t)) \quad (5)$$

Finally it is necessary take into account the contribution of the surface tension to the total pressure. This contribution is described by Laplace's Law.

$$P_{total}(r, t) = P_t^o(r, t) + \frac{2\gamma}{R_s(r)} + P_o \quad (6)$$

Where  $\gamma$  is the surface tension coefficient. However, a more detailed model, taking into account the chemical composition of the membrane, needs a more precise estimation for  $\gamma$  [11].  $R_s(r)$  is the local radius of curvature. This value is determined by the radius of the circumference with the best fit to the real membrane curvature in a local environment of the point  $r$ .  $P_o$  corresponds to other contributions to the total pressure, different from osmotic contributions, namely other substances presents inside or outside the membrane which can not cross it.

## SIMULATION MODEL

The reaction-diffusion system described by equations (1.1-1.6) can be calculated by using a discrete approximation using both discrete time and space (Schaff et al., 2001, Wiemar et al., 1994, Patankar, 1980). With such model it is possible to properly model the membrane behavior. Figure 2a indicates how this discrete approximation can be performed. The available space is divided into discrete elements of area  $dS = dx \cdot dy$ . Each discrete element is identified by its column and row (i,j). There are tree types of elements:

- Discrete internal elements, which cover all the area inside the membrane.
- Discrete external elements, which cover all the external area.

- Discrete membrane elements, which cover the membrane.

To construct the discrete approximation to the real membrane, the membrane elements must be in contact with internal elements and external elements, and all the elements must define a closed system. Not all the elements in contact with the membrane can be employed in this membrane approximation because can be in contact only with one of the internal or external elements, but not with both.

To perform the calculations, it is useful to separate the concentrations: for a discrete internal elements  $(i,j)$  at time  $t$  the concentration is  $\hat{c}_x^i(i,j,t)$  and for an external element is indicated as  $\hat{c}_x^e(i,j,t)$ , for the substance  $x$  (where  $x=\{G_1, G_2, S_1, S_2, G_0, G'_0, R, L\}$ ). These are the concentration values used in the finite differences approximation for equations (2). Depending on the discrete elements, the concentrations values must be:

- Discrete internal elements:  $\hat{c}_x^e=0$  y  $\hat{c}_x^i\neq0$
- Discrete external elements:  $\hat{c}_x^e\neq0$  y  $\hat{c}_x^i=0$
- Discrete membrane elements:  $\hat{c}_x^e\neq0$  y  $\hat{c}_x^i\neq0$

Each point of the membrane is crossed by different flows. If we use the discrete approximation to the membrane, instead to the real continuous membrane, we need to introduce some corrections in the discrete flow.

First, it is necessary to determine the normal direction to the membrane at each discrete membrane element. To do that, take a set of *characteristic points*  $Q_k$  along the real membrane with only one characteristic point per discrete membrane element. Initially the characteristic point for each discrete membrane element is chosen in the middle of the segment that crosses the discrete membrane element. The normal direction associated to the membrane element  $(i,j)$  is defined by the angle  $\Phi_{(i,j)}$  between the normal to the real membrane at the characteristic point and the horizontal axe (see figure 2a.).

When the calculations are performed on a discrete lattice, due to the diffusion process each element exchange molecules with just its nearest neighbours, as figure 2b shows. Let us indicate as  $g_{(i,j)-(l,m)}$  the exchanged flow between elements  $(i,j)$  and  $(l,m)$  if both are internal or external elements. If the element  $(i,j)$  belongs to a discrete membrane element the exchanged flow between them is  $g_{(i,j)-(l,m)} \cdot A_{(i,j)-(l,m)}$  with:

$$A_{(i,j)-(l,m)} = \begin{cases} \cos \Phi_{(i,j)} & \text{if } i = l \\ \sin \Phi_{(i,j)} & \text{if } j = m \end{cases} \quad (7)$$

In this situation, the calculus of the boundary conditions (3) must be corrected with (7).

## MEMBRANE DEFORMATION

The real membrane shape can be described by the locations of the characteristic points  $Q_k$ . Each one of these points has one membrane element associated in our approximation. The model assumes that at each one of these characteristic points the difference of concentrations at both sides is the same that the difference of concentrations  $\hat{c}_x^i - \hat{c}_x^e$ , for the substance  $x$ , associated to the discrete membrane element which contains the characteristic point. This difference of concentrations at both membrane sides creates an osmotic pressure. Under certain conditions these pressures are enough to deform the membrane. To simulate this effect it is necessary to assume that each characteristic point can change its position under these pressures. In a first approximation the displacement of each point is proportional to the total pressure described by (6).

$$Q_k(t + \Delta t) = Q_k(t) + b \cdot P_{total}(t, Q_k) \quad (8)$$

with  $b$  the proportionality constant and  $\Delta t$  the discrete time interval used in the CA calculus.

If, after the displacement, one *characteristic point*  $Q_k$  has a new location, different to its previous one, it is necessary to perform certain corrections in the concentration values. If at time  $t$  the location of the *characteristic point*  $Q_k$  is associated to the discrete element  $(i,j)$ , and at time  $t + \Delta t$  the new location of  $Q_k$  is associated to the discrete element  $(l,m)$ , and  $i \neq l$  or  $j \neq m$ , the new concentrations are:

$$\left. \begin{array}{l} \hat{c}_x^i((l,m), t + \Delta t) = \hat{c}_x^i((l,m), t + \Delta t) + \hat{c}_x^i((i,j), t + \Delta t) \\ \hat{c}_x^i((i,j), t + \Delta t) = 0 \end{array} \right\} \begin{array}{l} \text{if } (l,m) \text{ is an internal} \\ \text{discrete element.} \end{array} \quad (9)$$

$$\left. \begin{array}{l} \hat{c}_x^e((l,m), t + \Delta t) = \hat{c}_x^e((l,m), t + \Delta t) + \hat{c}_x^e((i,j), t + \Delta t) \\ \hat{c}_x^e((i,j), t + \Delta t) = 0 \end{array} \right\} \begin{array}{l} \text{if } (l,m) \text{ is an external} \\ \text{discrete element.} \end{array}$$

With the new characteristic point locations it is possible to regenerate the new shape of the membrane using a lineal interpolation. After this process it is necessary to define which discrete elements are internal, external or membrane elements again.

This model assumes that the membrane is continuous and closed at each instant. Due the displacements of the characteristic points it might be necessary to increase the number of discrete membrane elements to maintain the membrane closed and continuous. This situation corresponds to an increase of the real size of the membrane. The only mechanism to increase the membrane size is adding new building blocks  $M$  to the membrane, being produced by the metabolic reactions (1.5) and (1.6). If the size of the membrane is directly related to the number of blocks  $M$ , the production rate of the reactions (1.5) and (1.6) must be enough to ensure that, at each time the membrane size is the same as the membrane generated by interpolating between the different characteristic points.

A final rule is required to effectively generate a separation between two daughter cells. Since the membrane is actually a continuous medium, this model could not

reproduce the total break of the membrane into two independent closed membranes unless some additional change is introduced. The real break of the membrane into two independent membranes is a singularity due to the real membrane composition. This singularity can be introduced in the simulations. After a deformation process, the new membrane shape is determined by interpolating between the different *characteristic points* of the membrane. This interpolation is performed in a clockwise direction. Given one *characteristic point*  $Q_k$  all the others points  $Q_m$  have a weight values associated. These weight values are calculated by using a distribution:

$$W(d_{Q_m Q_k}) = \frac{-A}{(d_{Q_m Q_k})^{12}} + \frac{B}{(d_{Q_m Q_k})^6} \quad (10)$$

where  $d_{Q_k Q_m}$  is the distance between both points. This function has a behavior similar to Lennard-Jones potential, frequently employed to describe the boundary between lipids in a membrane. Figure 3 shows the weight profile used here. Given one characteristic point  $Q_k$  the interpolation will be performed between this point and the point  $Q_m$  with higher value of  $W(d_{Q_k Q_m})$  in the clockwise direction. Figures 4a and 4b show how this process can take place. In the figure 4a, with a spheroid shape, the interpolation process starts at the *characteristic point* labeled  $Q_i$  (this initial point it is arbitrary). The next point with higher weight value, in the clockwise direction, is  $Q_{i+1}$ , so the interpolation between  $Q_i$  and  $Q_{i+1}$  will be performed. The next interpolation will be between  $Q_{i+1}$  and  $Q_{i+2}$ , and so on. Figure 4b shows a membrane with a very high deformation. In the narrow neck zone the interpolation between  $Q_i$  and  $Q_{i+1}$  will be performed, but from  $Q_{i+1}$  the interpolation is possible with the point labeled  $Q_{i+2}$  or with the point labeled  $Q'_{i+2}$ , depending if  $W(d_{Q_{i+1}, Q_{i+2}}) > W(d_{Q_{i+1}, Q'_{i+2}})$  or  $W(d_{Q_{i+1}, Q'_{i+2}}) < W(d_{Q_{i+1}, Q_{i+2}})$ . If the interpolation is between  $Q_{i+1}$  and  $Q_{i+2}$  the simulation works with one deformed membrane, but if the interpolation is between  $Q_{i+1}$  and  $Q'_{i+2}$  the simulation assumes two closed membranes, one in the top half and other in the bottom half, in contact.

## RESULTS

The simulations show that, under certain conditions, the osmotic pressures can deform and in some cases eventually split the membrane. The osmotic pressure values of a substance depend on the different concentrations at each side of the membrane. These different concentrations basically depend on two parameters: permeability and different values of the diffusion coefficient inside and outside the membrane. In these simulations the diffusion coefficient is the same inside and outside, therefore the permeability becomes the fundamental parameter.

Table 1 shows the parameter values used in the simulations. The simulations have been performed on a 128x128 lattice of discrete elements. Initially, the metabolic centers  $E_1$  and  $E_2$  are located in two opposite positions in the membrane.  $G_1$  and  $G_2$  are produced in the metabolic centers  $E_1$  and  $E_2$  and diffuse through the membrane pushing it outside. Moreover,  $R$  and  $L$  come from the external medium and push the membrane towards inside. The substances  $G_1$ ,  $G_2$ ,  $G_0$  and  $R$  have the lower permeability values, therefore they give the greater contribution to the total osmotic pressures. The maximum production of  $G_0$  is located in the middle zone between  $E_1$  and  $E_2$ . Because  $G_0$  has a lower diffusion coefficient, its concentration is maximum in this middle zone. Reaction (1.3) stimulates a major penetration of  $R$  close to the zone where  $G_0$  is maximal.

Figure 5 show different moments of the evolution of the membrane-metabolism system. The pressures associated to  $G_1$  and  $G_2$  are favorable to the membrane expansion where these concentrations are higher. This occurs where  $E_1$  and  $E_2$  are located. On the other hand, the production of  $G'_0$  from  $R$  and  $G_0$  (reaction 1.4) stimulates the narrowing in the middle zone due the osmotic pressure associated to  $R$ . When the narrowing is enough, two independent membranes enter in contact. This qualitative change depends on the distance between the characteristic points in the narrowed zone, following (10).

During the expansion-narrowing process, the membrane size necessary to ensure that the membrane is continuous and closed increases. Figure 6 shows the coincidence between the size necessary to close the membrane across all the *characteristic points* and the real size of the membrane, calculated from the number of elements  $M$  produced by reactions (1.5) and (1.6).

## DISCUSSION

We have presented a minimal cellular model formed by a continuous closed membrane with some sort of simple metabolism inside. It has been shown that the effect of variable osmotic pressures, under certain conditions, can be a regulatory mechanism for the division process. These osmotic pressures are generated by the internal cellular metabolism, consistently with some old theoretical predictions (Rashevsky, 1960). The behavior of the membrane under metabolisms able to create variable osmotic pressures could be very relevant to the synthesis of artificial protocells synthesis, as well as for understanding some prebiotic scenarios, where the sophisticated division mechanisms of the current cells were not present. In this context, the set of reactions defining the internal metabolism can be arbitrarily generalized, thus opening the door for many different types of membrane-metabolism couplings.

The metabolism analyzed need two metabolic centers  $E_1$  y  $E_2$  adhered to the internal side of the membrane. These centers can just be two enzymes with the appropriate reaction centers able to catalyze several reactions simultaneously (two in our example). After cellular division, each daughter cell has only one metabolic center. At this point, the division process cannot start again without the replication of the metabolic center. This is a very important limitation to consider this model as a self-replication mechanism. However, our simulations suggest that a metabolism where the non-uniform concentration distribution arise form a spatiotemporal pattern (as in Turing patterns) without specifically located metabolic centers could be an efficient self-replication mechanism for minimal cells.

## References

- Alberts, B. et al. 2005. *Molecular Biology of the Cell*. 4<sup>th</sup> edition. Garland, New York
- Bozic, B., Svetina, S.. 2004. A relationship between membrane properties forms the basis of a selectivity mechanism for vesicle self-reproduction. *Eur. Biophys. J.* **33**: 565-571
- Hanczyc, M. M., and Szostak, J. W. 2003. Experimental Models of Primitive Cellular Compartments: Encapsulation, Growth, and Division. *Science* **302**, 618 - 622
- Hanczyc, M. M. and Szostak, J. W. 2004. Replicating vesicles as models of primitive cell growth and division. *Curr. Opin. Chem. Biol.* **8**, 660-664.
- Lodish, H. et al., 2005. *Molecular Cell Biology*. 4<sup>th</sup> edition. Freeman, New York.
- Maynard Smith, J., Szathmáry, E. 2001. *The Major Transitions in Evolution*. Oxford University Press.
- Morgan, J. J., Surovtsev, I. V., Lindahl, P. A. 2004. A framework for whole-cell mathematical modeling. *J. Theor. Biol.* **231**, 581-96.
- Munteanu, A. and Solé, R. V. 2005. Phenotypic Diversity and Chaos in Protocell Dynamics. *J. Theor. Biol.* In press.
- Noguchi, H., Takasu, M., 2002. Adhesion of nanoparticles to vesicles: a Brownian dynamics simulation. *Biophysical Journal*. **83**, 299-308
- Ono, N. and Ikegami, T. 1999. Model of Self-Replicating Cell Capable of Self-Maintenance. In: *Lecture Notes In Computer Science*; Vol. 1674, 399-406. Springer, London UK.
- Patankar, S., 1980. *Numerical Heat Transfer and Fluid Flow*. Taylor and Francis, Washington D.C.
- Rashevsky, N. 1960. *Mathematical Biophysics. Physico-matematical foundations of biology*. Vol I. Dover Publications, Inc. New York, USA.
- Rasmussen, R., Chen, L., Deamer, D., Krakauer, D. C., Packard, N. H., Stadler, P. F. and Bedau, M. A. 2004. Transitions from Nonliving to Living Matter. *J. Theor. Biol.* **303**, 963 - 965
- Schaff, J. C., Slepchenki, B. M., Yung-Sze Choi, Wagner, J., Resasco, D., Loew, L. M., 2001. Analysis of nonlinear dynamics on arbitrary geometries with the Virtual Cell. *Chaos* **11**, 115-131.
- Solé, R. V., Macía, J., Fellermann, H., Munteanu, A., Sardanyés, J. and Valverde, S. 2006. Models of protocell replication. In: *Protocells: bridging living and non-living matter*. Steen Rasmussen et al., editors. MIT Press.

Szostack W., Bartel, D. P. and Luisi, P. L. 2001. Synthesizing life. *Nature* **409**, 387-390

White, S. H., 1980. Small phospholipids vesicles: Internal pressure, surface tension, and surface free energy. *Proc. Natl. Acad. Sci. USA* **77**, 4048-4050.

Wiemar, J.R., Boon, J.P., 1994. Class of cellular automata for reaction-diffusion systems. *Phys. Rev. E* **49**, 1749-

## FIGURE CAPTIONS

**Figure 1.** Schematic representation of the minimal cell. The structure is formed by a closed continuous membrane. Adhered to the internal side of the membrane there are two enzymes  $E_1$  and  $E_2$ . These enzymes are the catalyst of a part of the metabolic reactions. When a molecule of  $R$  is in contact with  $E_1$  this molecule breaks into a pair of molecules  $G_1$ ,  $S_1$ . The same occurs when  $R$  is in contact with  $E_2$ . In this case  $R$  is broken into  $G_2$  and  $S_2$ .  $G_1$  and  $G_2$  produce  $G_0$ .  $G_0$  and  $R$  produce  $G'_0$ . Finally, the  $L$ -molecules are the precursors of the membrane building blocks  $M$ , being transformed in presence of  $E_1$  and  $E_2$ .

**Figure 2 (a)** Space discretization for the lattice model. The grid is formed by squares with a unit surface  $dS = dx \cdot dy$ . There are tree types of squares or *discrete elements*: *internal elements*, covering the internal space surrounded by the membrane, *external elements* for the area outside the membrane and *membrane discrete elements*. In **(b)** we indicate as  $g_{(k,q)-(l,m)}$  the specific flow exchanged between elements  $(k,q)$  and  $(l,m)$ , where the index  $(l,m)$  corresponds to different elements around  $(k,q)$ . When in the neighborhood there are *discrete membrane elements* this values of flow  $g_{(k,q)-(l,m)}$  must be corrected, because the flow which arrives to the discrete membrane elements do it along the normal direction defined by the angle  $\Phi_{(k,q)}$

**Figure 3. (a)** Membrane with a spheroid shape. The interpolation process starts at the *characteristic point* labeled A (this initial point it is arbitrary). The next point with higher weight value, in the clockwise direction, is B, so the interpolation between A and B will be performed. The next interpolation will be between B and C, and so on. **(b)** Here we show a membrane with a very high deformation. In the narrow neck zone there are two possibilities: the interpolation can be performed between B and C, if  $W(d_{BC}) > W(d_{BC'})$ , or between B and  $C'$  if  $W(d_{BC}) < W(d_{BC'})$ . In the first case there is only one deformed membrane. In the second case there are two membranes in contact.

**Figure 4.** Weight distribution between two membrane *characteristic points* plotted against their relative distance. This profile is similar to the so-called Lennard-Jones potential.

**Figure 5.** Spatiotemporal dynamics of the membrane-metabolism model. The expansion process takes place basically around the metabolic centers  $E_1$  and  $E_2$  due the osmotic pressures generated by  $G_1$  and  $G_2$ . Conversely, in the middle zone the effect of the osmotic pressure associated to  $R$  is dominant, and creates a narrowing effect. The plane

XY represents the space (as described by our lattice, discrete approximation). The vertical axis represents the concentration of  $G_1$  and  $G_2$ . The maxima are located around the two enzymes (metabolic centers)  $E_1$  and  $E_2$ .

**Figure 6.** Linear growth of membrane size over time. The symbols (●) indicate the membrane size needed to guarantee a closed, continuous membrane passing through all the characteristic points which define the membrane shape. The continuous line corresponds to the number of building blocks  $M$  presents in the membrane produced by the metabolic reactions (1.5) and (1.6).

**Table 1.** Parameter values for the rates of metabolic reactions and membrane deformations used in the simulations displayed in figure 5. The proportionality constant  $k_x$  for osmotic pressures calculations in equation (5) is the same for all substances.

Figure 1

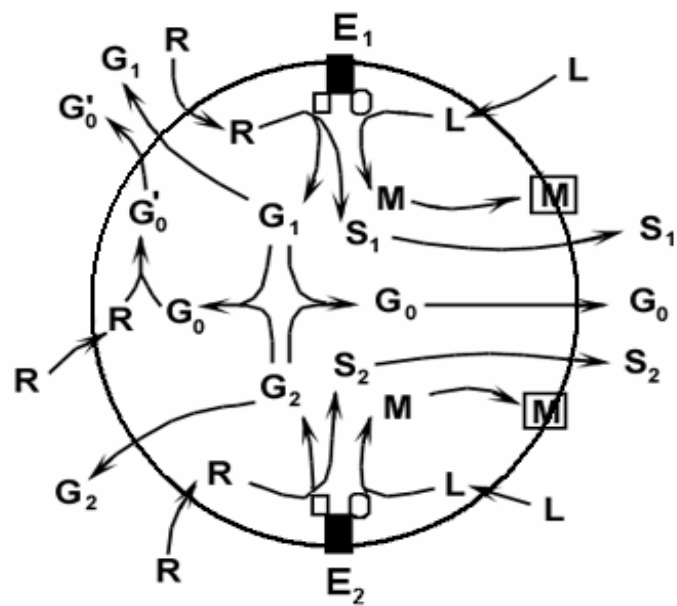


Figure 2a

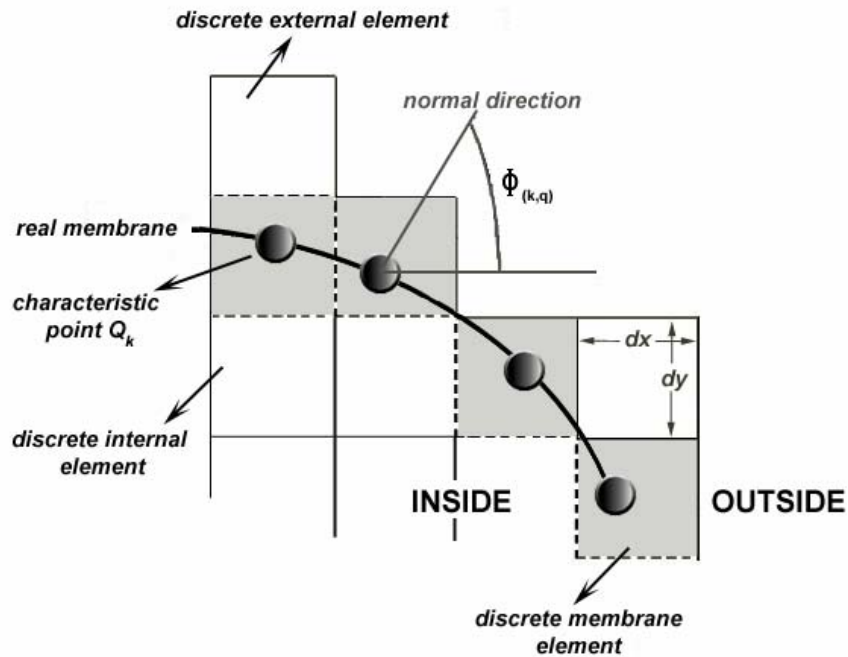
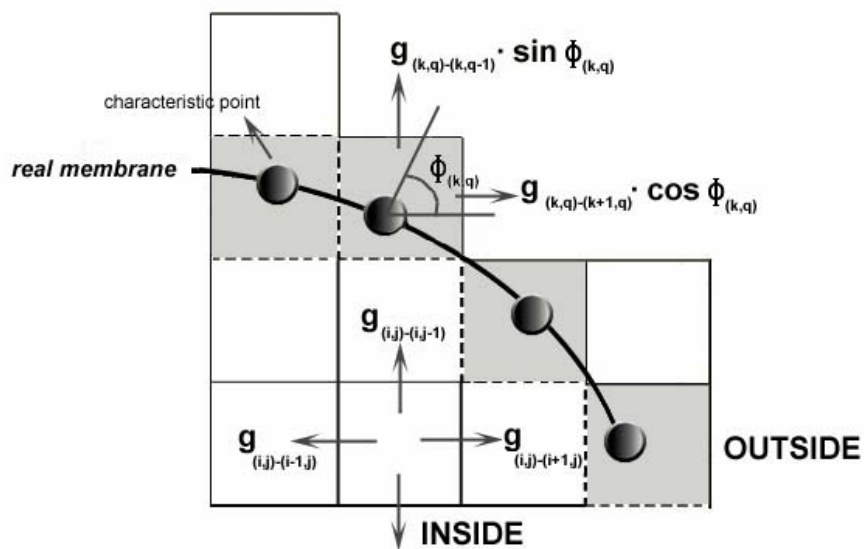


Figure 2b



**Figure 3**

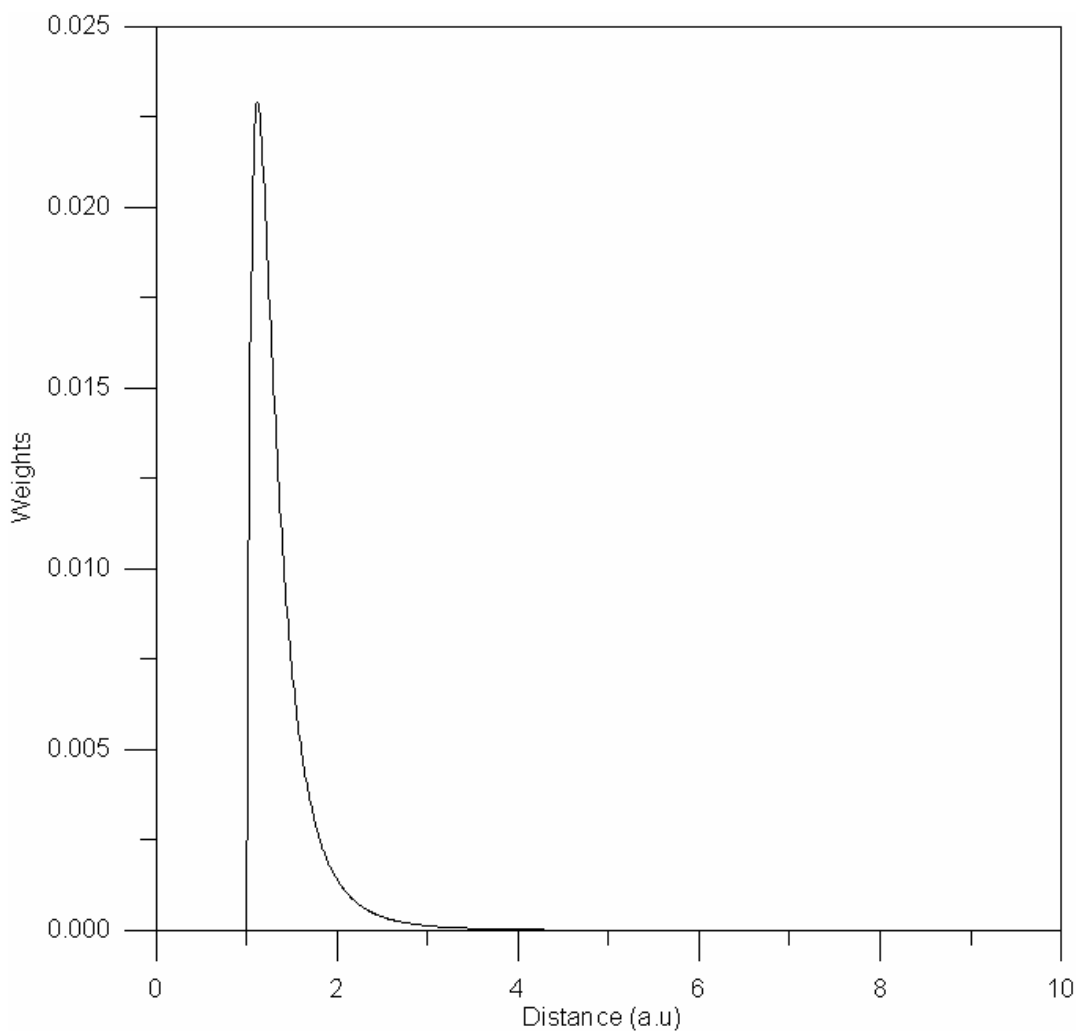
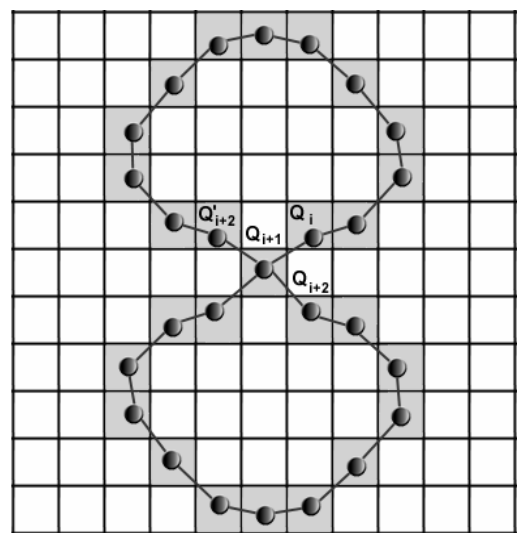
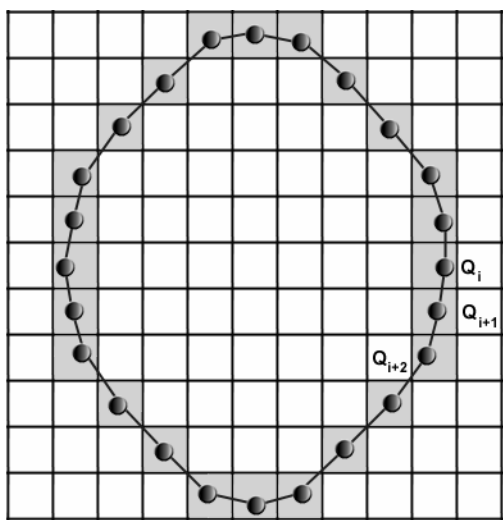
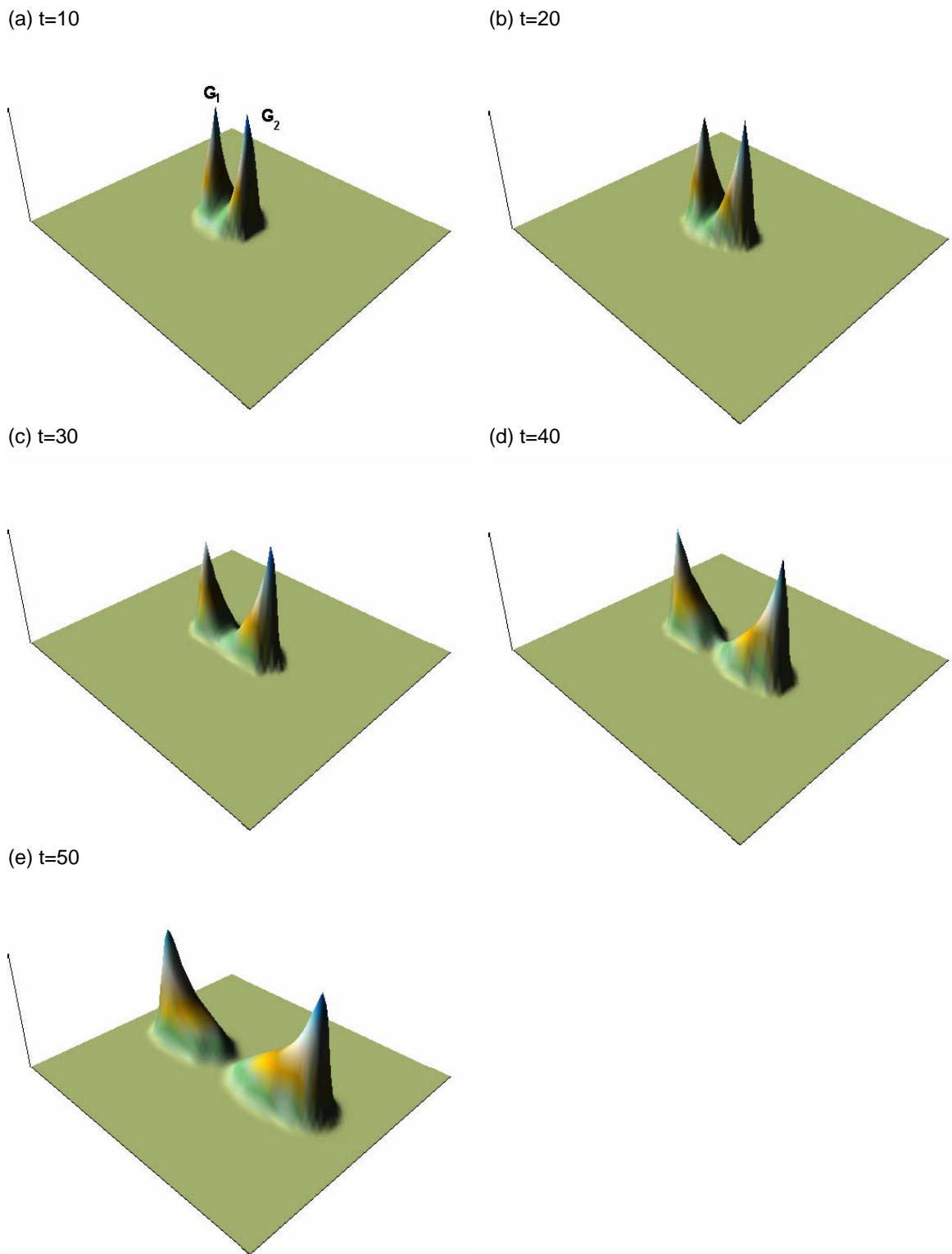


Figure 4a-b



**Figure 5.**



**Figure 6.**

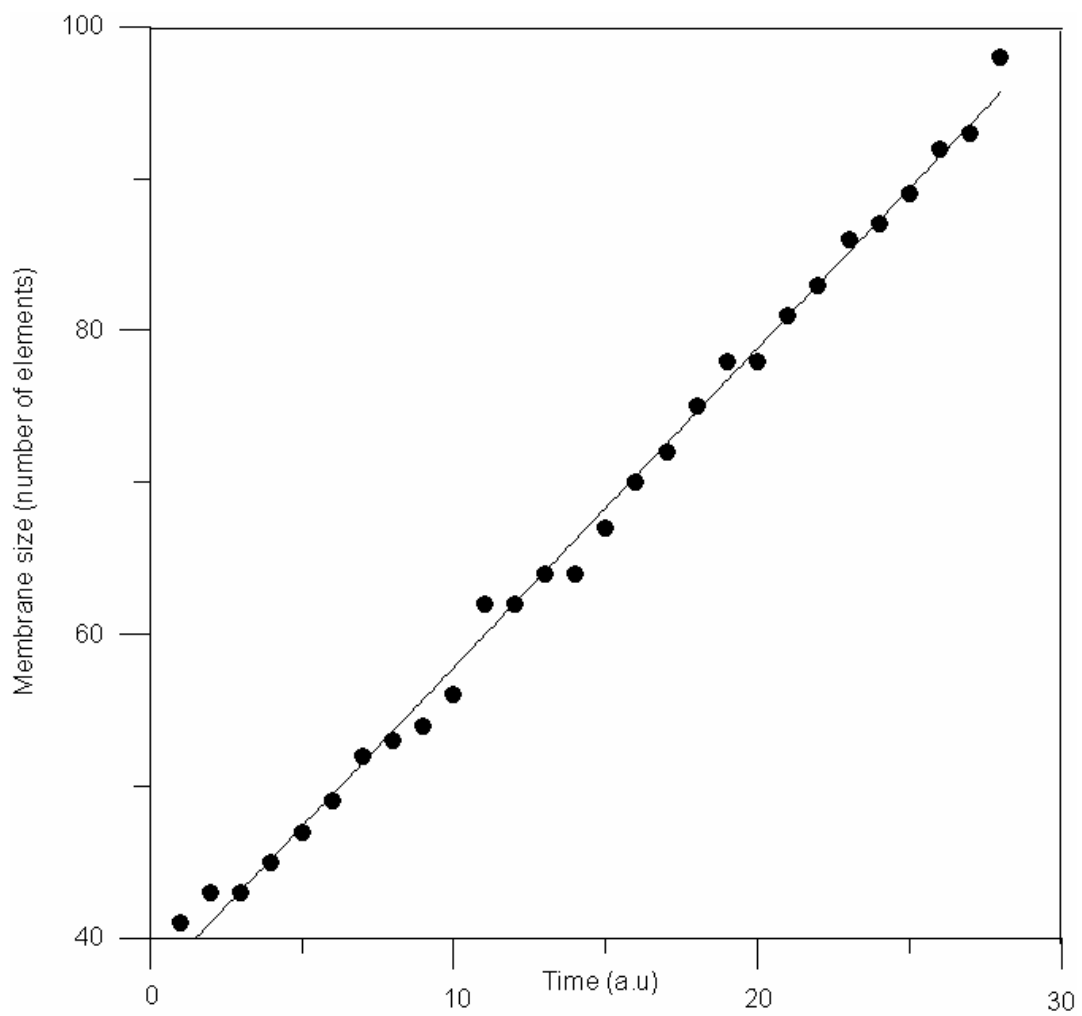


**Table 1.**

Parameter	Symbol	Value (a.u)
Kinetic constant	$k_1$	0.9
“	$k_2$	0.9
“	$k_3$	0.7
“	$k_{-3}$	$10^{-4}$
“	$k_4$	0.06
“	$k_{-4}$	$10^{-4}$
“	$k_5$	0.016
“	$k_6$	0.016
Permeability	$h_R$	0.015
“	$h_L$	0.03
“	$h_{G1}$	0.005
“	$h_{G2}$	0.005
“	$h_{S1}$	0.03
“	$h_{S2}$	0.03
“	$h_{G0}$	0.01
“	$h_{G'0}$	0.05
Diffusion coefficient	$D_R$	0.9
“	$D_L$	0.9
“	$D_{G1}$	0.9
“	$D_{G2}$	0.9
“	$D_{S1}$	0.9
“	$D_{S2}$	0.9
“	$D_{G0}$	0.2
“	$D_{G'0}$	0.9
Displacement proportionality constant	$b$	0.003
Substance contribution	$R_o$	50
Surface Tension Coefficient	$\gamma$	0.1
“	$L_o$	50